Supporting Information

Upconversion System with Quantum Dots as Sensitizer: Improved Photoluminescence and PDT Efficiency

Dan Song[†], Siyu Chi[†], Xin Li[†], Caixia Wang[‡], Zhen Li[‡], Zhihong Liu*[†]*

[†]Key Laboratory of Analytical Chemistry for Biology and Medicine (Ministry of Education), College of Chemistry and Molecular Sciences, Wuhan University, Wuhan 430072, China

[‡]College of Chemistry and Chemical Engineering, Hubei University, Wuhan 430062, China

Corresponding Author

*zhenli@whu.edu.cn

*zhhliu@whu.edu.cn

Materials. 1-Octadecene (ODE), oleic acid (OA), and 9,10-anthracenediyl-bis(methylene)dimalonic acid (ABDA) were purchased from Aladdin Reagent, Ltd. (Shanghai, China). Selenium powder (≥ 99.5%), 1-octanethiol (OT, ≥ 98.5%), 2,7-Dichlorodihydrofluorescein diacetate (DCFH-DA), Calcein-AM and silver acetate (AgAc) were obtained from Sigma Aldrich (St. Louis, MO, USA). The rest of the chemical reagents were supplied by the Sinopharm Chemical Reagent Co., Ltd. (Shanghai, China). All chemical reagents were analytical grade or higher and used without further purification. All aqueous solutions were prepared by ultrapure water (Mill-Q, Millipore, 18.25 MΩ resistivity). Mice were supplied by Wuhan Goodbio technology Co. Ltd. (Wuhan, China). All animal studies were performed in accordance with Animal Care and Use Committee of Wuhan University.

Instrumentations. The size and morphology of UCNPs and Ag_2Se QDs were characterized by a JEM-2010 transmission electron microscope with an acceleration voltage of 200 kV. The UV-vis-NIR absorption spectra were obtained on a UV-3600 ultraviolet-visible-infrared spectrophotometer (Shimadzu, Japan). The NIR luminescence spectra were measured through a Fluorolog-3 fluorescence spectrophotometer (Horiba Jovin Yvon Inc.) and the upconversion luminescence spectra were measured by a RF-5301 PC fluorometry (Shimadzu, Japan) with an external 808 nm CW laser (Beijing Hi-Tech Optoeletronic Co., China). Fourier transform infrared spectroscopy (FT-IR) tests were recorded on a NICOLET 5700 FTIR Spectrometer (Thermoelectron, USA), using the KBr pellet technique. X-ray photoelectron spectroscopy (XPS) spectra were performed on an ESCALAB 250xi X-ray Photoelectron Spectrometer (Thermo Scientific, US). Powder X-ray diffraction (XRD) patterns were recorded on a Bruker D8 Advanced X-ray diffractometer (Bruker axs) with a 2θ range from 10° to 80° with Cu Kα irradiation (k= 1.5406 Å). The fluorescence images were performed on a Zeiss Examiner LSM 780 multiphoton laser scanning confocal microscope (Carl Zeiss, Germany). The fluorescence lifetime was recorded on FLS980 spectrometer (Edinburgh Instrument). In vivo UCL images were acquired by Perkin Elmer IVIS Spectrum. All UV-Vis-NIR and fluorescence spectra in this experiment were obtained from solution measurements.

Supplementary Figures

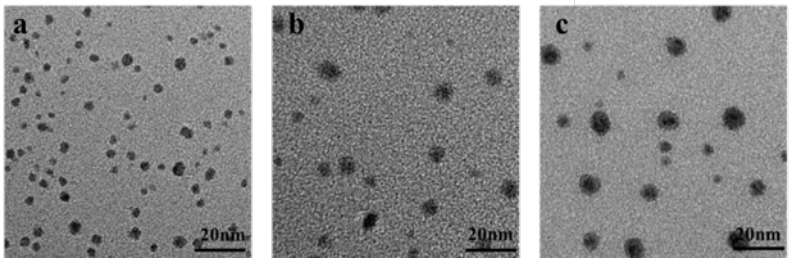

Figure S1. TEM images of Ag_2Se-810 (a), Ag_2Se-850 (b) and Ag_2Se-870 (c).

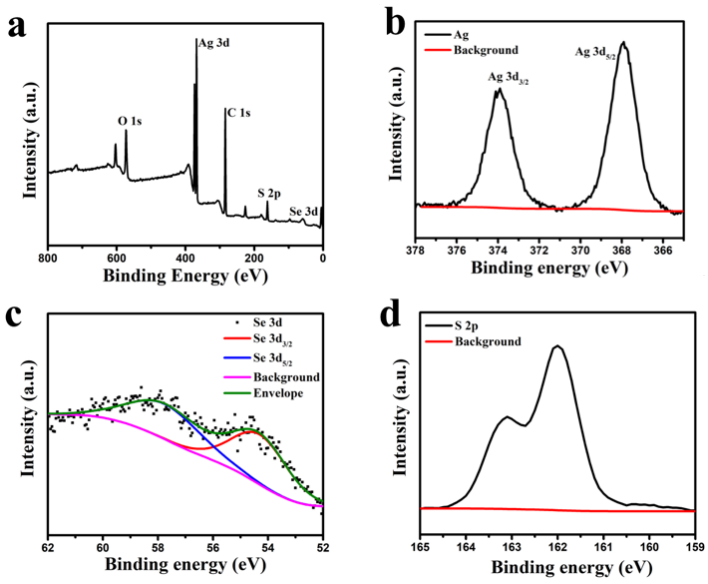

Figure S2. X-ray photoelectron spectroscopy (XPS) survey spectrum of Ag_2Se QDs (a), Ag 3d (b), Se 3d (c), S 2p (d). The signals assigned to Ag 3d orbitals (368 and 374 eV), and Se 3d orbitals (54.2 eV) confirmed the formation of Ag_2Se QDs.

	Absorption peak	Emission	ε_{808nm} (l g^{-1} cm^{-1})
1	810 nm	965 nm	0.21254
2	850 nm	975 nm	0.17621
3	870 nm	985 nm	0.13849

Table S1. Photophysical properties of the synthesized Ag_2Se QDs with different molar ratios of Ag to Se.

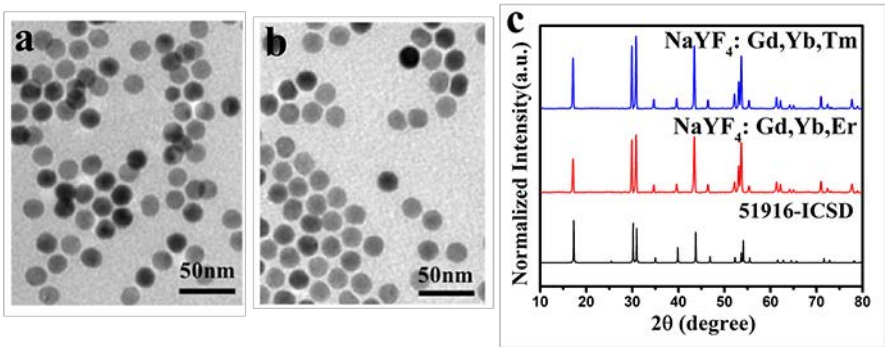

Figure S3. TEM images of the prepared $NaYF_4:Yb^{3+}/Gd^{3+}/Er^{3+}$ (a) and $NaYF_4:Yb^{3+}/Gd^{3+}/Tm^{3+}$ (b). c) X-ray diffraction (XRD) patterns of the prepared UCNPs.

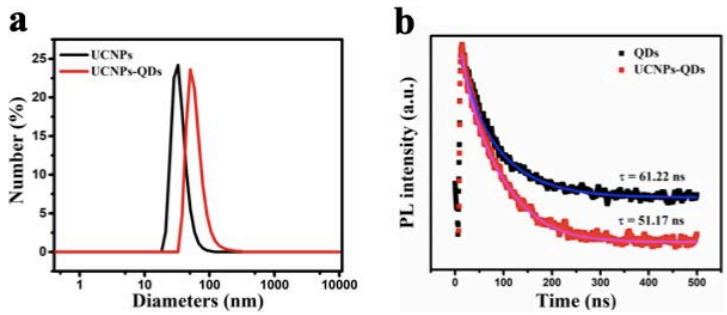

Figure S4. a) Hydrodynamic diameters of UCNPs before and after encapsulating with Ag_2Se QDs. b) Fluorescence lifetime of Ag_2Se QDs before and after encapsulating with UCNPs.

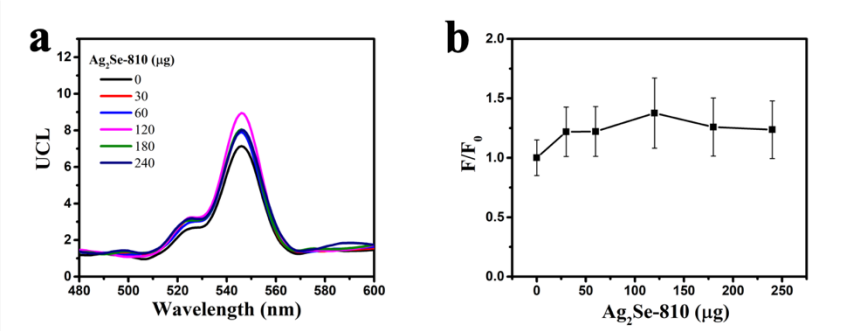

Figure S5. a) UCL spectra and b) the enhancement factor of $NaYF_4:Gd^{3+}/Er^{3+}$ capped with different amount of Ag_2Se-810 QDs. F and F_0 represent the UCL intensity at 545 nm with and without Ag_2Se QDs.

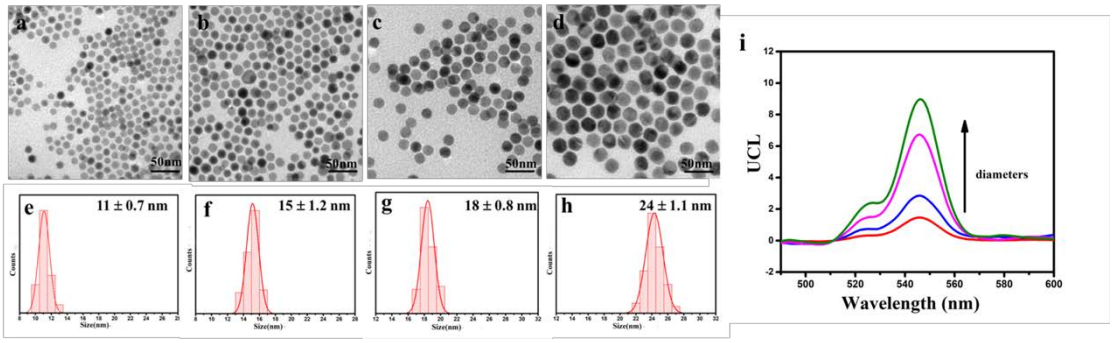

Figure S6. TEM images of $NaYF_4$:Yb,Gd,Er with different diameters (a-d) and their corresponding size distributions (e-h). i) UCL spectra of these four kinds of nanoparticles.

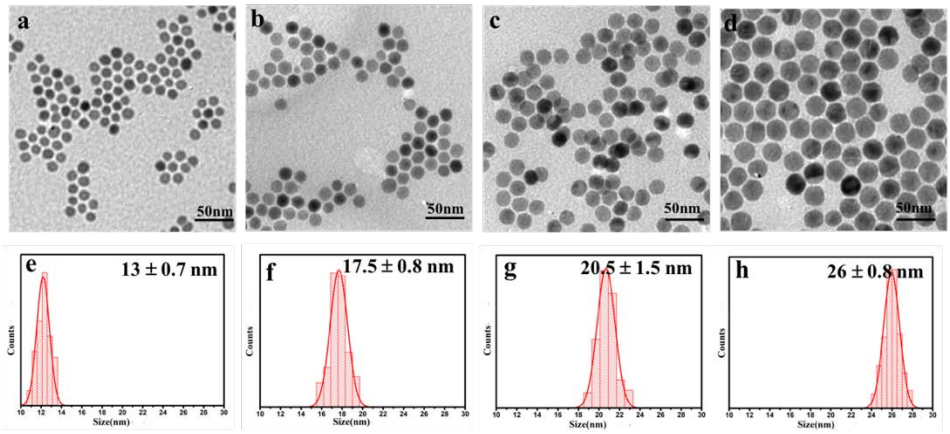

(A, ~1 nm shell)

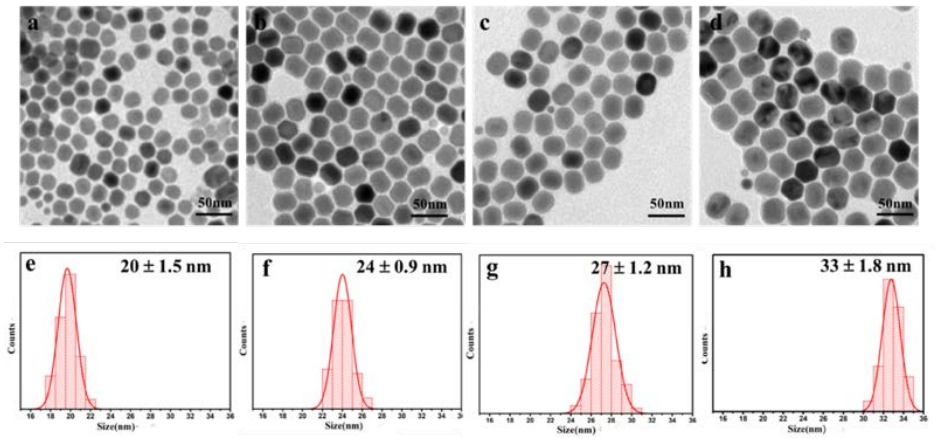

(B, ~4.5 nm shell)

Figure S7. TEM images of the $NaYF_4$:Yb,Gd,Er@$NaYF_4$ core-shell structures with different shell thickness, A) 1.0 nm shell, B) 4.5 nm shell, (a-d) with core diameter of 11, 15, 18, 24 nm, respectively, and their corresponding size distributions (e-h).

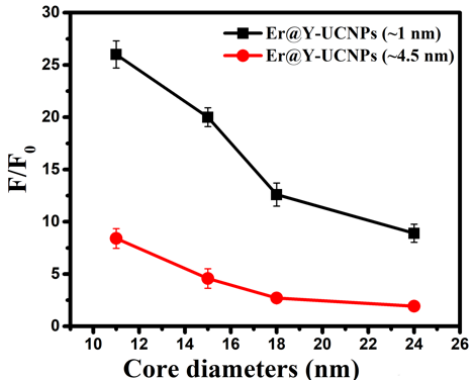

Figure S8. The UCL Enhancement factor of the eight UCNPs-QDs composites. F and F_0 represent the UCL intensity with/without Ag_2Se QDs in aqueous. Er@Y-UCNPs refers to $NaYF_4$:Yb,Gd,Er@$NaYF_4$.

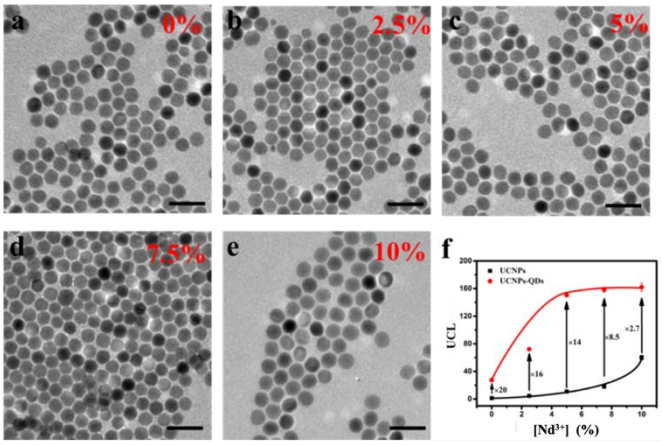

Figure S9. TEM images of UCNPs ($NaYF_4$:Yb,Gd,Er@$NaYF_4$:x%Nd) with different doping concentrations of Nd^{3+} (a-e) and corresponding UCL of these UCNPs before and after co-encapsulating with Ag_2Se-810 QDs (f). Scale bar: 50 nm.

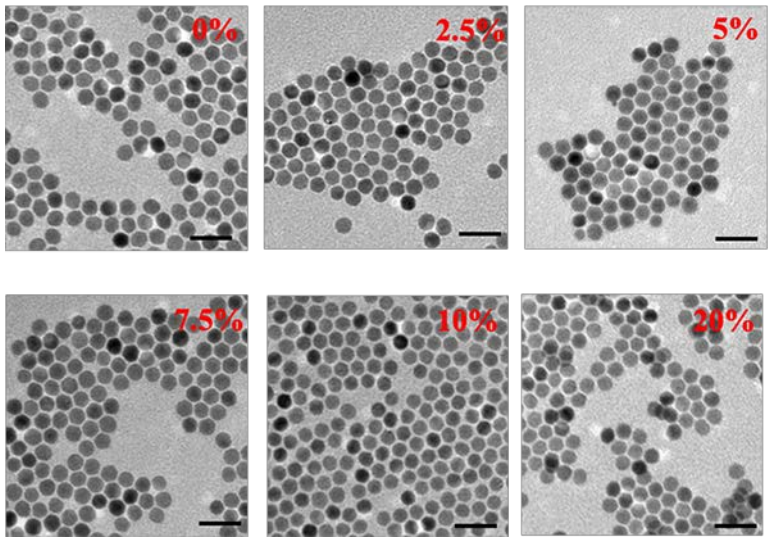

Figure S10. TEM images of UCNPs ($NaYF_4$:Yb,Gd,Er@$NaYF_4$:5%Nd,x%Yb) with different doping concentrations of Yb^{3+} in the shell layer. Scale bar: 50 nm.

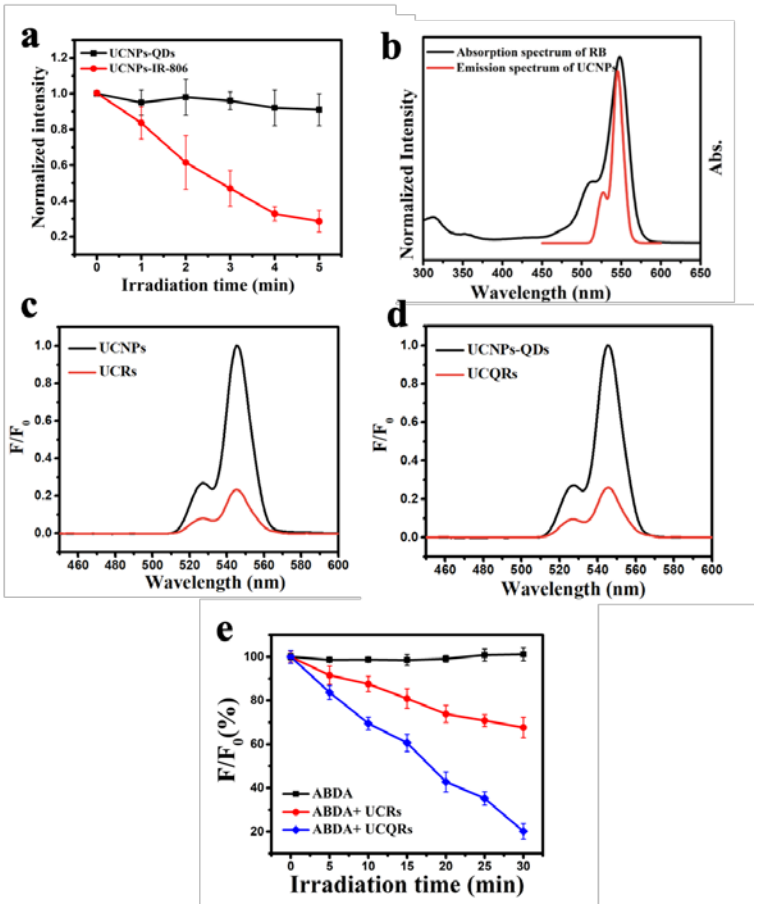

Figure S11. a) Normalized UCL intensity of UCNPs-QDs and UCNPs-IR-806 after 808-nm laser irradiation with a power density of 3.15 W/cm^2 for different time. b) Emission of UCNPs matches well with the absorption band of RB. c, d) Normalized UCL spectra of UCNPs and UCNPs-QDs before and after co-encapsulating with RB. The structure of the UCNPs is $NaYF_4$:Yb,Gd,Er@$NaYF_4$:5%Nd,7.5%Yb. e) Relative fluorescence intensity of ABDA at 400 nm as a function of irradiation time in the presence of UCRs or UCQRs. Control group is the ABDA probe itself under 808 nm laser irradiation (3.15 W/cm^2).

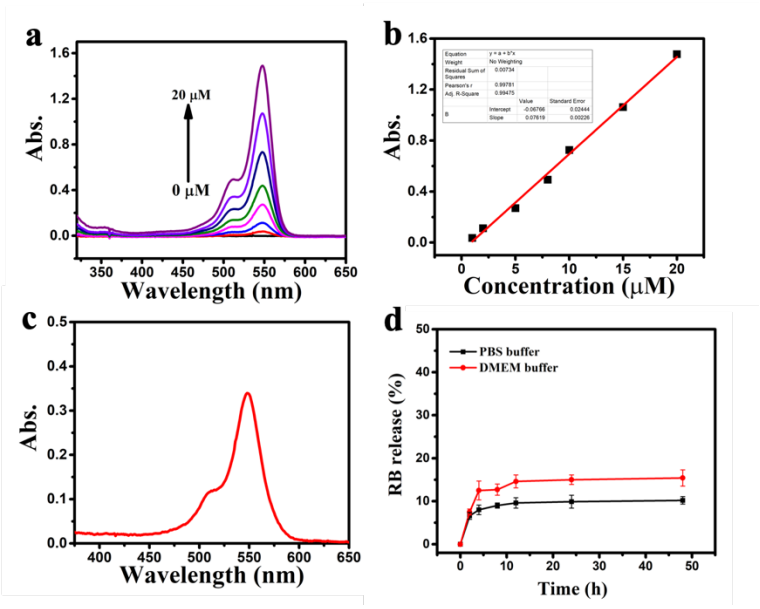

Figure S12. a) UV-Vis spectra of RB in PBS at various concentrations (0-20 μM). b) The plot of absorbance at 545 nm against the concentration of RB. The molar absorption coefficient of RB is 7.619×10^4 L·mol^{-1}·cm^{-1} as calculated from the plot. c) Absorption spectrum of the loaded RB of UCQRs (0.1 mg/mL). d) The percentage of released RB from UCQRs after incubation for different time in PBS buffer (pH=7.4, 10 mM) and DMEM medium with10% fetal calf serum.

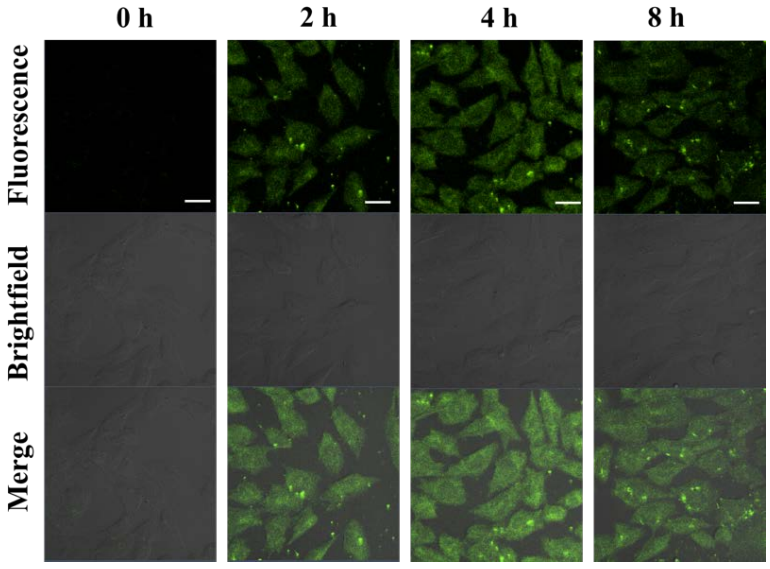

Figure S13. CLSM images of HeLa cells incubated with UCQRs for 0, 2, 4 and 8 h. Images were collected at 500-560 nm. Scale bar: 20 μm.

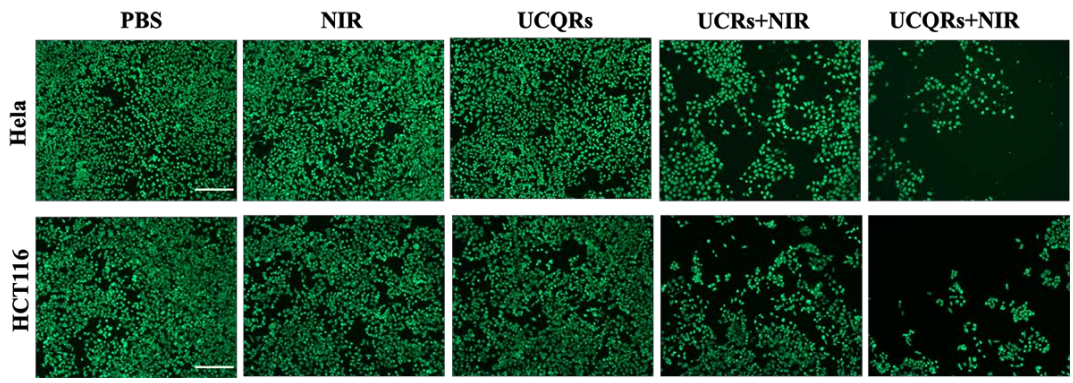

Figure S14. Calcein-AM staining assay for living cells. HeLa cells and HCT116 cells were treated with different conditions (PBS, only 808-nm laser irradiation, only UCQRs, UCRs or UCQRs combined with 808-nm laser irradiation). The excitation wavelength was 490 nm, and the emission was collected at 500—540 nm. Scale bar: 200 μm.

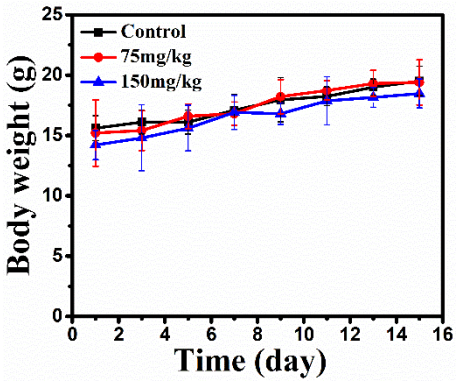

Figure S15. Body weight of healthy mice after receiving different dose of UCQRs.

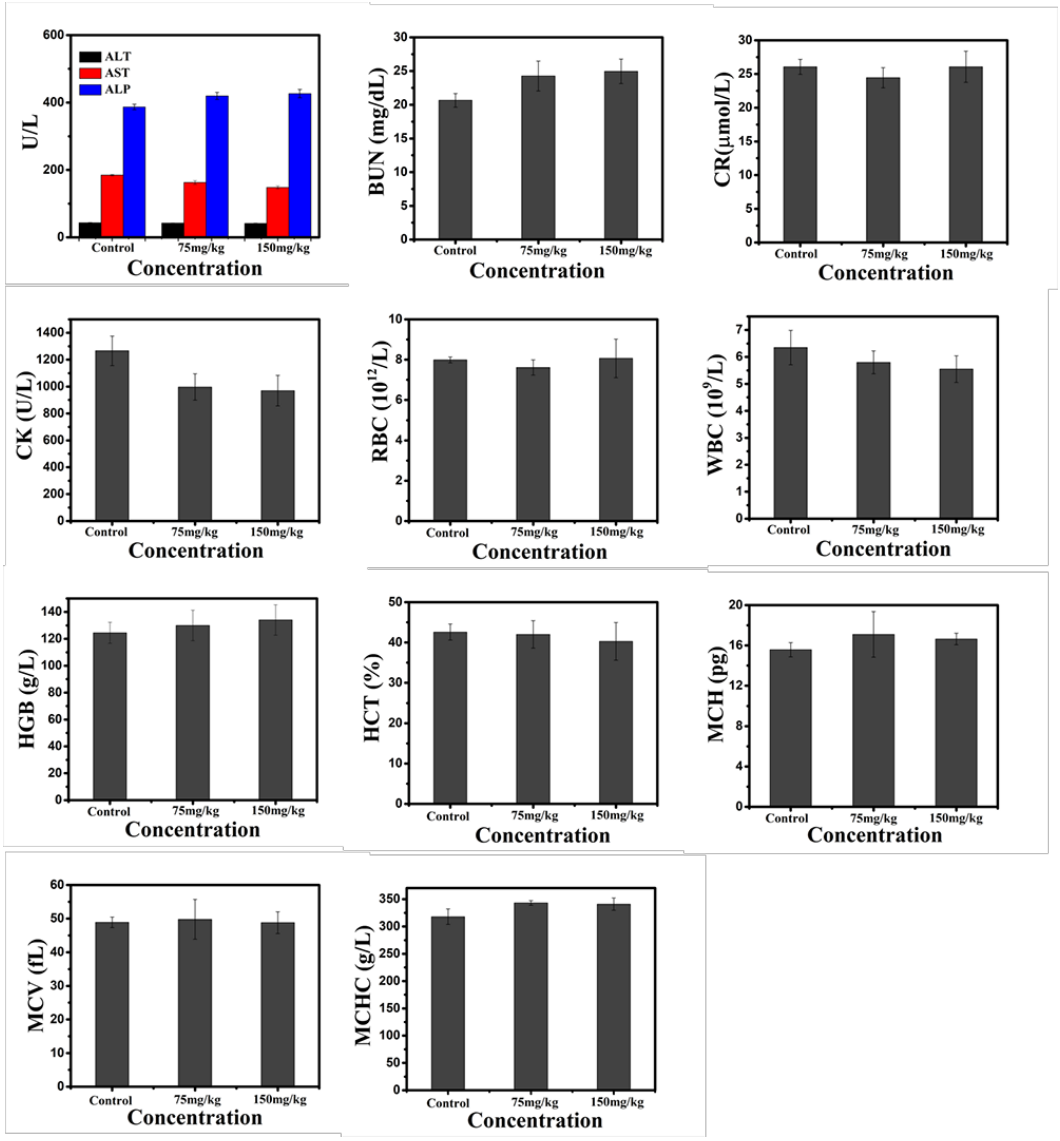

Figure S16. Blood routine and serum biochemical levels of mice after receiving different doses of UCQRs, including alanine aminotransferase (ALT), aspartate aminotransferase (AST), alkaline phosphatase (ALP), blood urea nitrogen (BUN), creatinine (CR), Creatine Kinase (CK), red blood count (RBC), white blood count (WBC), hemoglobin (HGB), hematocrit (HCT), mean corpuscular hemoglobin (MCH), mean corpuscular volume (MCV) and mean corpuscular hemoglobin concentration (MCHC).

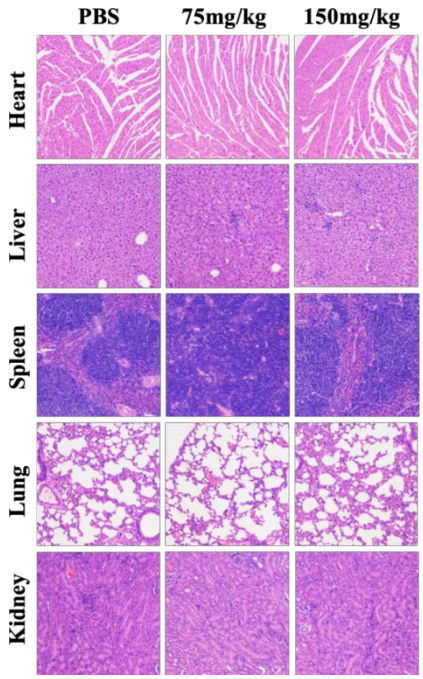

Figure S17. H&E staining images of major organs (healthy mice) after receiving different dose of UCQRs.

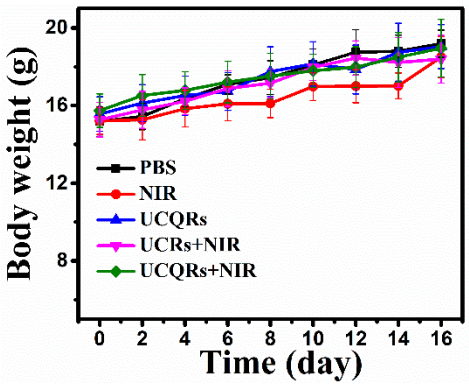

Figure S18. Body weight of LLC tumor bearing mice after receiving different treatments.

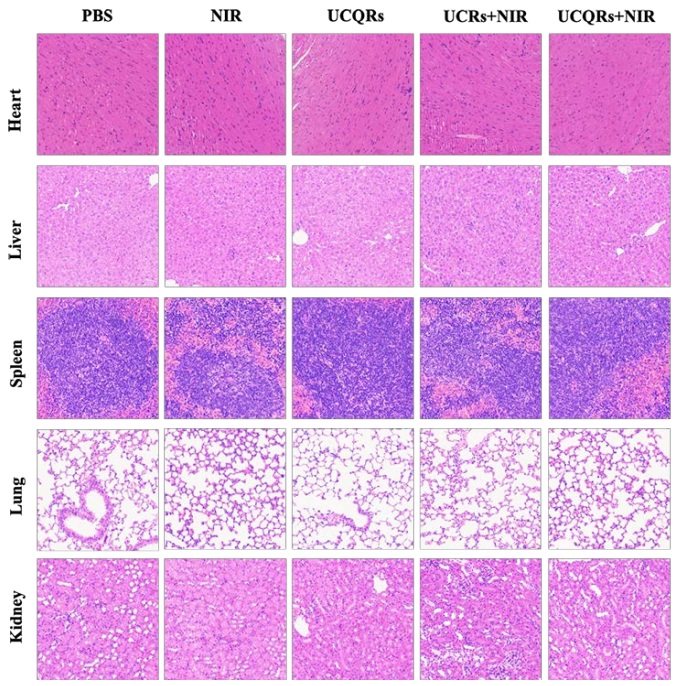

Figure S19. H&E stain of major organs (LLC tumor bearing mice) after receiving different treatments.

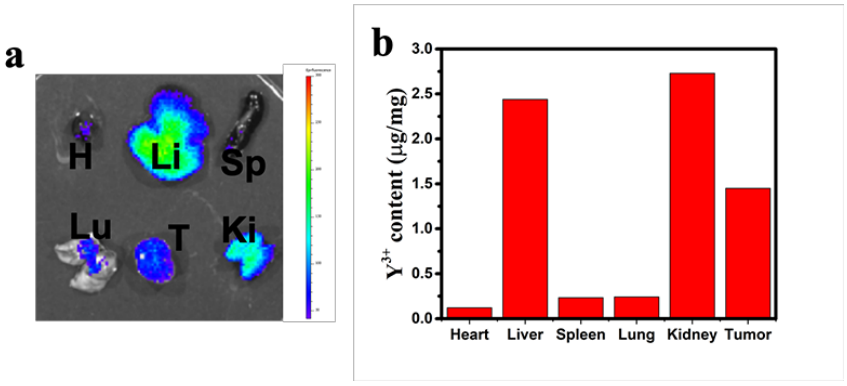

Figure S20. The UCL image (a) and Y^{3+} contents (b) of organs of the 4T1 tumor bearing mouse injected with UCQRs.

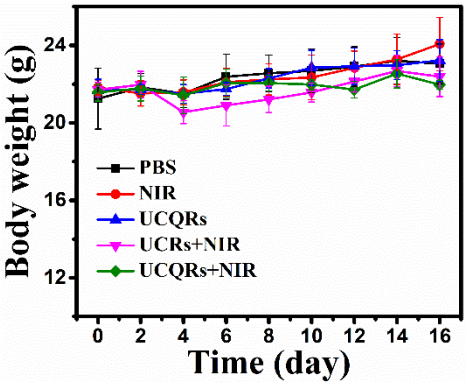

Figure S21. Body weight of 4T1 tumor bearing mice after receiving different treatments.

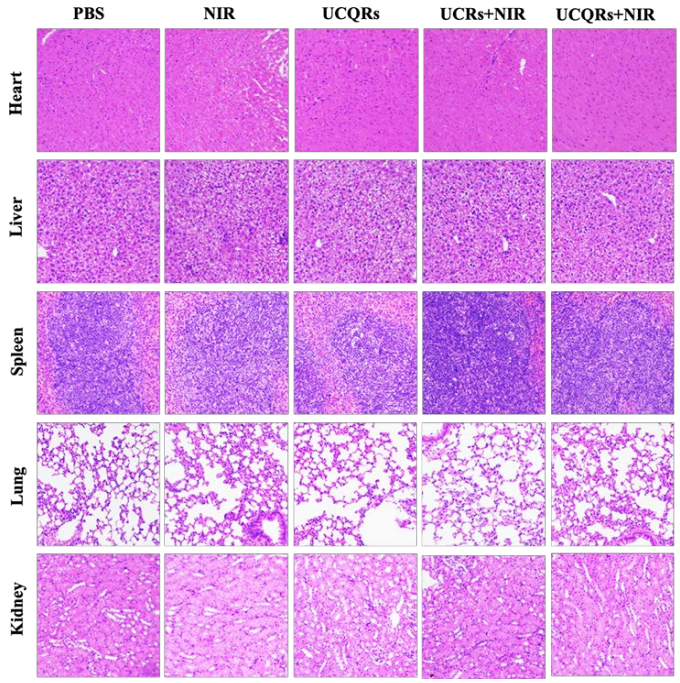

Figure S22. H&E stain of major organs (4T1 tumor bearing mice) after receiving different treatments.